Analyst

ROYAL SOCIETY OF CHEMISTRY

PAPER

View Article Online
View Journal

Cite this: DOI: 10.1039/d1an00028d

A hairpin probe-mediated DNA circuit for the detection of the *mecA* gene of *Staphylococcus aureus* based on exonuclease III and DNAzyme-mediated signal amplification†

Jiafeng Pan,[a,b] Dongqin Bao,[c] Enhu Bao[c] and Junhua Chen *[b]

Received 7th January 2021,
Accepted 12th April 2021

DOI: 10.1039/d1an00028d

rsc.li/analyst

A simple, highly sensitive biosensor for *S. aureus* detection is becoming increasingly important in human health and safety. In this work, a hairpin probe-mediated DNA circuit for the detection of the *mecA* gene of *S. aureus* was reported cascading Exo III-assisted cycling signal amplification and the DNAzyme-mediated cleavage reaction. In the presence of the target *mecA* gene, the recognition and hybridization between HP1 and *mecA* can trigger Exo III and DNAzyme-mediated signal amplification and further release numerous ATMND, resulting in an enhanced fluorescence response, which serves as a response signal for the fluorescence detection of *mecA* gene. This biosensor enables the sensitive and specific detection of the *mecA* gene, showing a linear response ranging from 1 fM to 1 nM with a detection limit of 0.5 fM. Moreover, this fluorescence assay has been applied for the analysis of clinical samples with satisfactory recovery. Importantly, this universal platform can be further extended for the analysis of other targets by alternating the corresponding recognition unit, which holds much promise in point-of-care testing for bacterial analysis.

Introduction

Hospital-acquired infections have been leading causes of death worldwide.[1–4] Of the many *Staphylococcus aureus* (*S. aureus*) antibiotic variants, methicillin-resistant *S. aureus* (MRSA) presents a major public health problem.[5] Due to the resistance of all penicillins and other β-lactam antibiotics, MRSA is the main causative agent for severe community-acquired nosocomial and hospital infections.[6] The mechanism of antibiotics resistance in MRSA is based on incorporation with *mec* DNA, including *mecA*, a gene encoding penicillin-binding protein 2a (PBP 2a). The group of infections arising due to MRSA has been associated with a substantial increase in morbidity and mortality rates.[7,8] Early detection of MRSA is critical to control the infection and improve patient outcomes.[9] Therefore, the development of a simple, highly sensitive biosensor for *S. aureus* detection is urgently needed.

Conventional clinical methods for the detection of *S. aureus* include antibiotic susceptibility testing (AST),[10,11] polymerase chain reaction (PCR),[12–14] matrix-assisted laser desorption ionization-time-of-flight mass spectrometry (MALDI-TOFMS),[15–17] enzyme-linked immune-absorbent assay (ELISA),[18] and surface plasmon resonance (SPR) methods.[19] Even though these methods have advanced sensitivity and specificity for microbiology detection, they require laborious sample treatment, long operation time and complex instruments, hindering their application for point-of-care (POC) testing. Thus, there is a pressing demand for convenient, rapid, and low-cost diagnostic techniques for *S. aureus* analysis. Recently, various detecting techniques have been successfully applied for *S. aureus* diagnosis, including colorimetry,[20–25] electrochemistry,[26–29] and fluorescence.[30–32] However, the sensitivity of these technologies is unsatisfactory, which limits the clinical application.

In order to overcome these limitations, exonuclease III (Exo III)-assisted signal amplification has been applied to amplify response signals.[33,34] Unlike other tool enzymes, Exo III is a sequence-independent enzyme that does not need the specific recognition site, which could specifically cleave the double stranded DNA (dsDNA) when substrates have a blunt or recessed 3-terminus.[35,36] The cleavage activity toward single stranded DNA (ssDNA) or dsDNA with a protruding 3′-end is

[a]College of Bioscience and Biotechnology, Hunan Agricultural University, Changsha 410128, China
[b]National-Regional Joint Engineering Research Center for Soil Pollution Control and Remediation in South China, Guangdong Key Laboratory of Integrated Agro-environmental Pollution Control and Management, Institute of Eco-environmental and Soil Sciences, Guangdong Academy of Sciences, Guangzhou 510650, China. E-mail: 222chenjunhua@163.com, jhchen@soil.gd.cn
[c]Shuyang Hospital Affiliated to Xuzhou Medical University, Suqian 223800, China

†Electronic supplementary information (ESI) available: Supplementary data (Fig. S1–S4 and Tables S1, S2). See DOI: 10.1039/d1an00028d

limited.[37,38] Therefore, Exo III provides a versatile platform for the amplified detection of nucleic acids.

In this work, a hairpin probe-mediated DNA circuit for the detection of the *mecA* gene of *S. aureus* was developed cascading Exo III and DNAzyme-mediated signal amplification. When the target *mecA* was introduced, the recycle I process was triggered in the signal amplification reaction, releasing the enzyme strand DNA 1. With the co-factor Mg^{2+}, the free DNA 1 that acted as the active DNAzyme could induce the recycle II process, leading to the cleavage reaction toward the substrate ATMND-HP2 complex, releasing the caged ATMND and sensitively detecting the characteristic *mecA* gene. Because of the remarkable amplification efficiency of Exo III and the Mg^{2+}-dependent DNAzyme, the assay was ultrasensitive, resulting in the detection of trace levels of the *mecA* gene as low as 0.5 fM.

Experimental

Materials and reagents

Exo III was bought from Takara (Dalian, China). 2-Amino-5,6,7-trimethyl-1,8-naphthyridine (ATMND) was purchased from Enamine (Ukraine). All other reagents and materials were of analytical grade and obtained from Sigma-Aldrich (St. Louis, Mo). Milli-Q purified water (18.2 MΩ cm) was used to prepare the buffer solution.

All HPLC-purified sequences were purchased from Sangon Biotech Co., Ltd (Shanghai, China) and listed as follows:

mecA gene: 5′-ATTGGGATCA-TAGCGTCATT-3′

HP1: 5′-GGGGACTCCGAGCCGGACGAAGTTGGTTTTTTTG-AGT CCCCTGATCCCAAT-3′

HP2: 5′-CGCCGCCAACTrAGGTCCCCTTCGCCGTTTTTTT-3′

M1: 5′-ATTGGGAACATAGCGTCATT-3′

M2: 5′-ATTGGCAACATAGCGTCATT-3′

M3: 5′- ATTCGCAACATAGCGTCATT -3′

NC: 5′-TGCCGCTCATCCGCCACATA-3′

Assay procedure

All of the oligonucleotides were dissolved in 20 mM Tris-HCl buffer solution (pH 7.5, 150 mM NaCl, 50 mM KCl, and 20 mM $MgCl_2$). Before *mecA* gene detection, the hairpin probe 1 (HP1) was heated to 95 °C for 5 min and allowed to cool to room temperature. The hairpin probe 2 (HP2) probe and ATMND dye with a stoichiometric ratio of 2 : 1 were first mixed, heated to 90 °C for 5 min, and then cooled down to room temperature to form a stable ATMND-HP2 complex. For the detection of the *mecA* gene, 200 nM HP1 was incubated with different concentrations of the *mecA* gene at 25 °C for 30 min in the presence of 20 U Exo III. Subsequently, the 500 nM ATMND-HP2 complex was introduced into the above solution and incubated at room temperature for 45 min. The fluorescence spectra were recorded from 378 to 520 nm (E_x = 356 nm, E_m = 400 nm). The fluorescence measurements were measured using a SpectraMax i3x (Molecular Devices, the U.S.).

To investigate the selectivity of this biosensor for the specific detection, 10 nM *mecA* gene and 10 nM other mutations, including a single-base mismatched DNA (M1), a two base mismatched DNA (M2), a three base mismatched DNA (M3), and the non-complementary DNA (NC) were evaluated under the same assay conditions.

Analysis of real samples

All human serum samples were filtered with a 0.22 μm microfiltration membrane to remove the insoluble particles. Different concentrations of the *mecA* gene spiked in the real samples were quantified using our circuit. The concentrations of the *mecA* gene spiked in the real samples using the proposed method were compared with those acquired by quantitative real-time PCR (qPCR), which was performed using the following procedures: 95 °C for 3 min, followed by 40 cycles of 95 °C for 3 s, 60 °C for 30 s. Quantitative analysis was performed by combining DNA with SYBR Green I.

Results and discussion

Strategy for *mecA* gene monitoring

The principle of a hairpin probe-mediated DNA circuit for the detection of the *mecA* gene of *S. aureus* is illustrated in

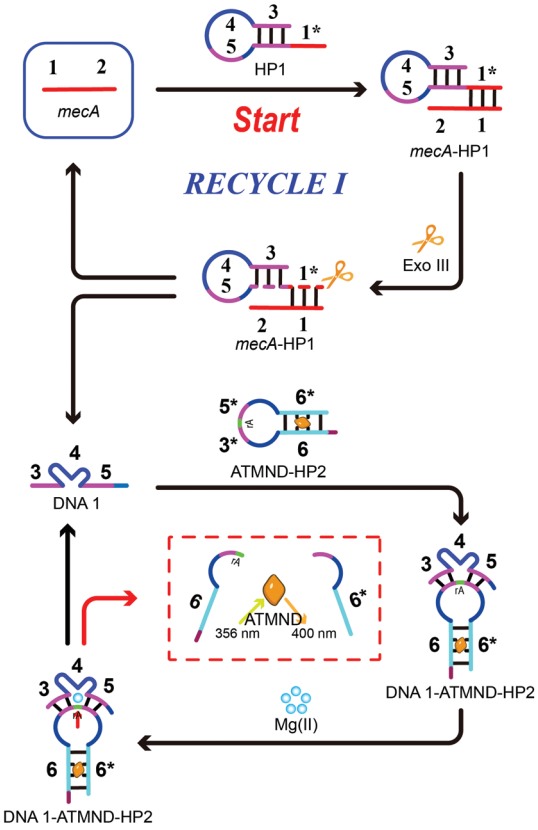

Scheme 1 Schematic illustration of a hairpin probe-mediated DNA circuit for the detection of the *mecA* gene of *Staphylococcus aureus* based on exonuclease III and DNAzyme-mediated signal amplification.

Scheme 1. Typically, all hairpin probes are duplex DNA with a 3′-overhang end. HP1 includes the enzyme strand. The fluorescent small molecule ATMND can selectively bind to a cytosine (C) at a C–C mismatch in double-stranded DNA with high affinity *via* the strong π-π stacking interaction, resulting in the quenching of its fluorescence.[39,40] HP2 with two functional sections has been elaborately designed for the test, which contains a C–C mismatch in the stem for ATMND binding and the ATMND-HP2 complex forming, and the substrate strand at the ring for DNAzyme-mediated signal amplification.[41–43] Exo III is applied for recycling the *mecA* gene, as well as to successively release DNA 1 for signal amplification. The reason for selecting Exo III as the amplifying unit is because it is a sequence independent enzyme which could provide a versatile platform for the amplified detection of the *mecA* gene at room temperature.[44] When the *mecA* is introduced, it hybridizes with domains 1* of HP1 to form the partial duplex (*mecA*-HP1 complex) through the Watson–Crick base-pairing interaction. In this case, Exo III is able to bind to duplex regions and catalyze the stepwise hydrolysis of mononucleotides from the 3′-ends of HP1. After the duplex is fully consumed, the *mecA* and DNA1 are released. The free *mecA* can automatically hybridize with other undigested HP1 and then trigger a new cycle (recycle I). On the basis of the autonomous cycles, large amounts of DNA1 can be produced to achieve Exo III-assisted signal amplification.

Furthermore, the products of Exo III-assisted signal amplification (DNA1) can bind synergistically with domains 3* and 5* of the ATMND-HP2 complex to form the stabilized supramolecular structure (DNA 1-ATMND-HP2). In the presence of the co-factor Mg^{2+}, DNA 1 that served as the activated DNAzyme can cleave continually the substrate ATMND-HP2 complex, leading to the dehybridization of the HP2 stem region (owing to the significant decrease in its melting temperature) and then releasing ATMND into solution, resulting in an enhanced fluorescent signal for *mecA* detection.[40] In the absence of *mecA*, all hairpins with a protruding 3′-end are resistant to the cleavage by Exo III. As a result, ATMND is caged in the stem of HP2 and only the background can be detected.

Feasibility study

To verify the feasibility of the hairpin probe-mediated DNA circuit, the fluorescence emission spectra were obtained under different assay conditions. As shown in Fig. 1, due to the high fluorescence quantum yield, the free ATMND showed a strong fluorescence signal (black line). The addition of HP2 to ATMND solution led to a significant decrease in fluorescence intensity (magenta line), indicating the quenching of ATMND and the formation of the ATMND-HP2 complex.[41] The obvious fluorescence response cannot be obtained in the presence of HP1 and Exo III (blue line), implying that Exo III-assisted cycling signal amplification and DNAzyme-mediated cleavage reaction were inhibited. When the *mecA* gene was added to the above solution, a significant enhancement of the fluorescence signal was achieved (red line), indicating that the binding between *mecA* and HP1 initiated Exo III-assisted cycling signal amplification, yielding numerous DNA 1. The products of DNA 1 further triggered the DNAzyme-mediated cleavage reaction, releasing ATMND with fluorescence recovery. These results clearly demonstrated that our DNA circuit can be utilized for the amplified detection of the target *mecA* gene.

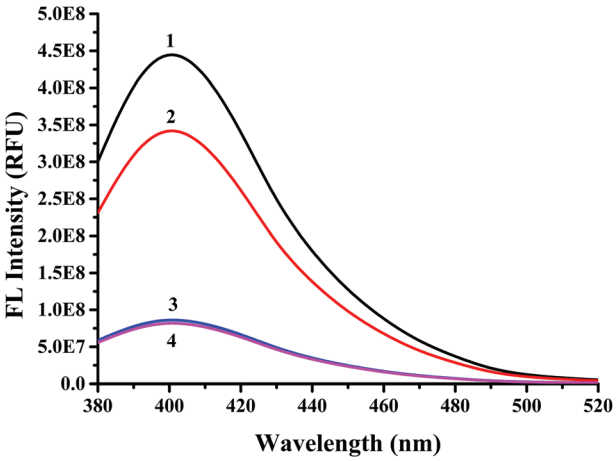

Fig. 1 Fluorescence emission spectra of the sensing system under different control conditions: (1) 500 nM ATMND, (2) 10 nM *mecA* + 200 nM HP1 + 500 nM ATMND + 500 nM HP2 + 20 U Exo III, (3) 200 nM HP1 + 500 nM ATMND + 500 nM HP2 + 20 U Exo III, (4) 500 nM ATMND + 500 nM HP2.

Optimization of the experimental conditions

Several key parameters (*e.g.*, the reaction temperature, the reaction time of Exo III-assisted signal amplification, Exo III dosage, and the cleavage time of DNAzyme) that could affect the analytical performance of the DNA circuit were investigated. In this work, the reaction temperature plays a crucial role in the sensing process. It not only affects the stability of hairpin probes, but also the cleavage activity of Exo III. The effect of reaction temperature on the response of the biosensor was optimized by detecting 10 nM *mecA* gene at different temperatures (4 °C, 25 °C, 37 °C, and 45 °C). The blank sample (without *mecA* gene) at each temperature was tested under the same conditions. As shown in Fig. S1,† the fluorescence signal increased accordingly with the increase of the temperature from 4 to 37 °C. However, the response signal decreased when further increasing the temperature to 45 °C (cyan histogram in Fig. S1†). This is probably because the catalytic ability of Exo III is restrained over the optimal temperature (37 °C) and even becomes inactivated at 45 °C. Also, the higher temperature may affect the conformation of hairpin probes, resulting in the rising background (gray histogram in Fig. S1†). In order to obtain the best signal-to-background ratio (S/N) (red line in Fig. S1†), 25 °C was considered to be the optimum reaction temperature. As shown in Fig. S2,† the fluorescence signal of the sensor containing 10 nM *mecA* gene rapidly reached its plateau when the reaction time was 30 min, which suggests that Exo III-assisted signal amplification was completely achieved. Thus, 30 min was selected as the optimum reaction

time. In addition, the effect of the enzyme dosage was also investigated on the basis of the fluorescence response toward the detection of 10 nM target gene. As depicted in Fig. S3,† the response signal increased with the enhancement of Exo III dosage and reached a platform after 20 U. Therefore, 20 U was chosen for further experiments. Furthermore, the cleavage time of the DNAzyme was optimized. As shown in Fig. S4,† the fluorescence signal gradually increased with increasing cleavage time and resulted in a stable value after 45 min, indicating that the cleavage reaction of the DNAzyme was completely finished and the caged dye ATMND in H2 was almost released to produce the fluorescence signal. Thus, 45 min was set as the optimal reaction time.

Analytical performance of the biosensor

The proposed biosensor was applied for the quantitative detection of the target gene *mecA* under the optimized assay conditions (Fig. S1–S3, ESI†). As displayed in Fig. 2A, the fluorescence intensities increased continuously with increasing concentration of *mecA* from 0 to 10 nM. From Fig. 2B, the fluorescence response showed a good linear relationship with the logarithm of *mecA* concentrations from 1 fM to 1 nM, and the regression equation was $F_{400} = 1.17 \times 10^8 + 3.56 \times 10^7 \lg C$ (R^2 = 0.99) with a detection limit of 0.5 fM (S/N = 3). For clinical diagnosis, regardless of the level of *mecA*, a positive result can be taken as the clinical decision. The sensitivity of the DNA circuit for *mecA* detection was compared with other biosensors (Table S1, ESI†). The results showed that the sensitivity of the circuit was comparable or even superior to some previously reported methods for *mecA* detection.

To evaluate the selectivity of the DNA circuit, 10 nM *mecA* mutations, including a single-base mismatched DNA (M1), a two base mismatched DNA (M2), a three base mismatched DNA (M3), and the non-complementary DNA (NC), were employed as interfering agents for the test. As depicted in Fig. 3, the fluorescence intensity of our proposed biosensor for 10 nM *mecA* gene is about 3.54×10^8 RFU. For the target with M1, M2 and M3, the fluorescence intensity decreased to 2.01×10^8 RFU, 1.46×10^8 RFU, and 0.89×10^8 RFU, respectively. The fluorescence intensity for NC and the blank sample is about 0.86×10^8 RFU. These data indicated that the fluorescence intensity was almost the same as the blank test when more than three mutated bases existed in the target. For real sample analysis, there are at least three different base variations in the gene between *S. aureus* and other pathogens.[45] Thus, our designed biosensor exhibited good selectivity and can effectively distinguish *S. aureus* and other pathogens.

Real sample analysis

The application of the DNA circuit was evaluated by performing a recovery test in actual clinical samples. Different concentrations of *mecA* were spiked into serum samples and detected using the as-proposed biosensor. As shown in Table S2 (ESI†), the satisfactory recovery and the relative standard derivation (RSD) were in the range 94%–105.4% and 4.3%–5.9%, respectively, indicating that the possible interference from the serum

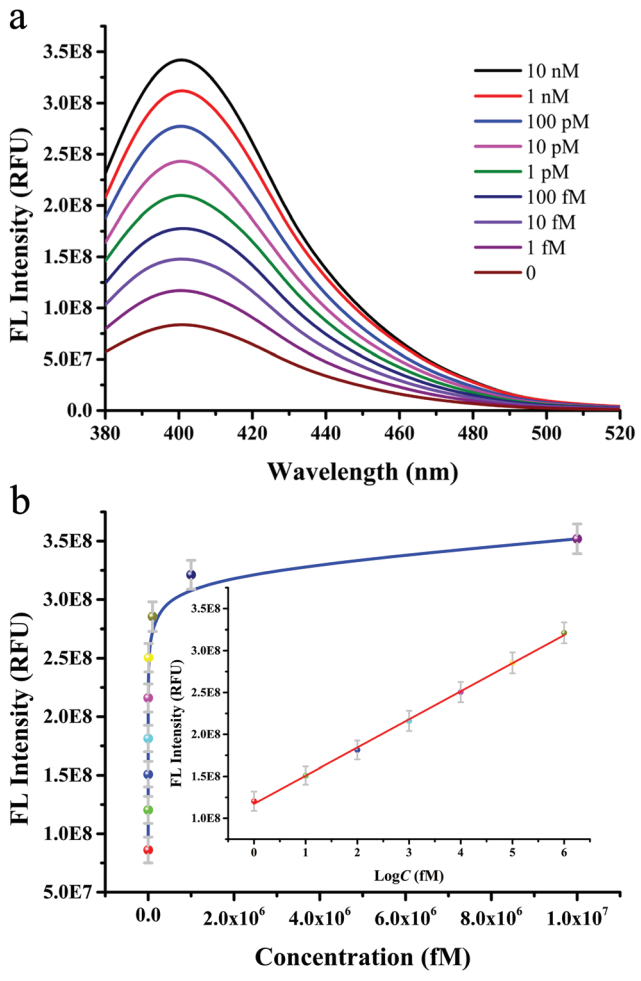

Fig. 2 (a) Fluorescence emission spectra of the sensing system in the presence of *mecA* concentrations. (b) Correlation of the fluorescence intensity at 400 nm with the *mecA* concentrations. The error bars are standard derivation obtained from three independent experiments.

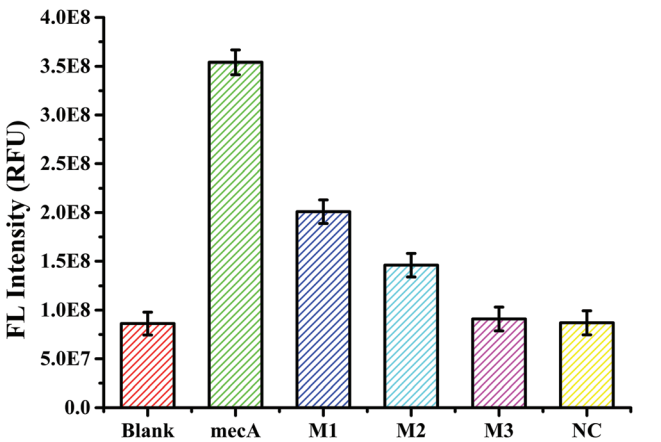

Fig. 3 Specificity investigation of the sensing platform for *mecA* against other mutations. *mecA*, 10 nM; other mutations, 10 nM. The error bars are standard derivation obtained from three independent experiments.

sample to the circuit was negligible. Moreover, the concentration of *mecA* in the spiked serum samples was further certified by the qPCR method. The data revealed that no significant difference existed between the values measured using the proposed fluorescence biosensor and qPCR, confirming the accuracy of the developed sensor for detecting the target *mecA*. These results demonstrated that our fabricated biosensor is reliable for *mecA* detection in clinical samples.

Conclusions

In conclusion, a hairpin probe-mediated DNA circuit for the detection of the *mecA* gene of *S. aureus* was developed cascading Exo III-assisted cycling signal amplification and the DNAzyme-mediated cleavage reaction. Briefly, HP1 was employed to recognize the target *mecA* gene. The binding between HP1 and *mecA* initiated Exo III and DNAzyme-mediated signal amplification, releasing numerous ATMND molecules, which results in an enhanced fluorescence response for *mecA* detection. This biosensor enables the sensitive and specific detection of the *mecA* gene, presenting a linear range from 1 fM to 1 nM with a detection limit of 0.5 fM. Furthermore, this fluorescence assay has been applied for the analysis of clinical samples with satisfactory recovery and RSD. Importantly, this universal platform can be further extended for the analysis of other targets by alternating the corresponding recognition unit, which holds great potential as point-of-care testing tools for bacterial analysis.

Conflicts of interest

There are no conflicts to declare.

Acknowledgements

This work was supported by the Guangdong Basic and Applied Basic Research Foundation (2021A1515012192).

Notes and references

1 S. Y. C. Tong, J. S. Davis, E. Eichenberger, T. L. Holland and V. G. Fowler, *Clin. Microbiol. Rev.*, 2015, **28**, 603–661.
2 K. A. Rodvold and K. W. McConeghy, *Clin. Infect. Dis.*, 2014, **58**, S20–S27.
3 S. R. Harris, E. J. Feil, M. T. G. Holden, M. A. Quail, E. K. Nickerson, N. Chantratita, S. Gardete, A. Tavares, N. Day, J. A. Lindsay, J. D. Edgeworth, H. de Lencastre, J. Parkhill, S. J. Peacock and S. D. Bentley, *Science*, 2010, **327**, 469–474.
4 C. Chang, J. Chern, M. Chen, K. Huang, C. Chen, Y. Yang and S. Wu, *J. Am. Chem. Soc.*, 2015, **137**, 267–275.
5 K. U. Jansen, C. Knirsch and A. S. Anderson, *Nat. Med.*, 2018, **24**, 10–19.
6 M. Rubab, H. M. Shahbaz, A. N. Olaimat and D. H. Oh, *Biosens. Bioelectron.*, 2018, **105**, 49–57.
7 J. M. Soriano, G. Font, J. C. Moltó and J. Mañes, *Trends Food Sci. Technol.*, 2002, **13**, 60–67.
8 K. Zhang, J. A. McClure and S. Elsayed, *J. Clin. Microbiol.*, 2005, **43**, 5026–5033.
9 S. O. Kelley, *SLAS Technol.*, 2017, **22**, 113–121.
10 W. Chan, B. S. F. Tang, M. V. Boost, C. Chow and P. H. M. Leung, *Biosens. Bioelectron.*, 2014, **53**, 105–111.
11 L. Xu, W. Liang, Y. Wen, L. Wang, X. Ynag, S. Ren, N. Jia, X. Zuo and G. Liu, *Biosens. Bioelectron.*, 2018, **99**, 424–430.
12 R. You, Z. Gui, Z. Xu, M. E. Shirtliff, G. Yu, X. Zhao, L. Shi, B. Li, J. Su and L. Li, *Afr. J. Microbiol. Res.*, 2012, **6**, 7131–7133.
13 H. M. Manukumar and S. Umesha, *Sci. Rep.*, 2017, **7**, 1–16.
14 A. Huletsky, P. Lebel, J. Picard, M. Bernier, M. Gagnon, N. Boucher and M. G. Bergeron, *Clin. Infect. Dis.*, 2005, **40**, 976–981.
15 Z. Du, R. Yang, Z. Guo, Y. Song and J. Wang, *Anal. Chem.*, 2002, **74**, 5487–5491.
16 K. A. Jackson, V. Edwards-Jones, C. W. Sutton and A. J. Fox, *J. Microbiol. Methods*, 2005, **62**, 273–284.
17 V. Edwards-Jones, M. A. Claydon, D. J. Evason, J. Walker, A. J. Fox and D. B. Gordon, *J. Med. Microbiol.*, 2000, **49**, 295–300.
18 S. S. Oh, K. Plakos, X. Lou, Y. Xiao and H. T. Soh, *Proc. Natl. Acad. Sci. U. S. A.*, 2010, **107**, 14053–14058.
19 H. Zhang, X. Ma, Y. Liu, N. Duan, S. Wu, Z. Wang and B. Xu, *Biosens. Bioelectron.*, 2015, **74**, 872–877.
20 Z. Zhang, Y. Guan, M. Li, A. Zhao, J. Ren and X. Qu, *Chem. Sci.*, 2015, **6**, 2822–2826.
21 H. Yang, M. Xiao, W. Lai, Y. Wan, L. Li and H. Pei, *Anal. Chem.*, 2020, **92**, 4990–4995.
22 Y. Zhang, W. Tan, Y. Zhang, H. Mao, S. Shi, L. Duan, H. Wang and J. Yu, *Biosens. Bioelectron.*, 2019, **142**, 111570.
23 P. Liu, L. Han, F. Wang, V. A. Petrenko and A. Liu, *Biosens. Bioelectron.*, 2016, **82**, 195–203.
24 P. Liu, Y. Wang, L. Han, Y. Cai, H. Ren, T. Ma, X. Li, V. A. Petrenko and A. Liu, *ACS Appl. Mater. Interfaces*, 2020, **12**, 9090–9097.
25 J. Zhou, R. Fu, F. Tian, Y. Yang, B. Jiao and Y. He, *ACS Appl. Bio. Mater.*, 2020, **3**, 6103–6109.
26 C. R. Nemr, S. J. Smith, W. Liu, A. H. Mepham, R. M. Mohamadi, M. Labib and S. O. Kelley, *Anal. Chem.*, 2019, **91**, 2847–2853.
27 U. Farooq, M. W. Ullah, Q. Yang, A. Aziz, J. Xu, L. Zhou and S. Wang, *Biosens. Bioelectron.*, 2020, **157**, 112163.
28 A. Abbaspour, F. Norouz-Sarvestani, A. Noori and N. Soltani, *Biosens. Bioelectron.*, 2015, **68**, 149–155.
29 Y. Liu, Y. Wei, Y. Cao, D. Zhua, W. Ma, Y. Yu and M. Guo, *Biosens. Bioelectron.*, 2018, **117**, 830–837.
30 S. Y. Yi, J. Jeong, K. E. Kim, K. Park and Y. B. Shin, *ACS Infect. Dis.*, 2020, **6**, 215–223.
31 N. Bhardwaj, S. K. Bhardwaj, J. Mehta, K. H. Kim and A. Deep, *ACS Appl. Mater. Interfaces*, 2017, **9**, 33589–33598.

32 Y. Huang, H. Zhang, X. Chen, X. Wang, N. Duan, S. Wu, B. Xu and Z. Wang, *Biosens. Bioelectron.*, 2015, **74**, 170–176.
33 Q. Li, D. Zhou, J. Pan, Z. Liu and J. Chen, *Analyst*, 2018, **143**, 5670–5675.
34 Y. Sun, C. Zhao, Z. Yan, J. Ren and X. Qu, *Chem. Commun.*, 2016, **52**, 7505–7508.
35 C. Li, H. Chen, J. Hu and C. Zhang, *Chem. Sci.*, 2020, **11**, 5724–5734.
36 X. Qu, D. Zhu, G. Yao, S. Su, J. Chao, H. Liu, X. Zuo, L. Wang, J. Shi, L. Wang, W. Huang, H. Pei and C. Fan, *Angew. Chem., Int. Ed.*, 2017, **56**, 1855–1858.
37 S. Liu, X. Yu, J. Wang, D. Liu, L. Wang and S. Liu, *Anal. Chem.*, 2020, **92**, 9764–9771.
38 X. Huang, S. Wu, H. Hu and J. Sun, *ACS Sens.*, 2020, **5**, 2636–2643.
39 J. Pan, Q. Li, D. Zhou and J. Chen, *Talanta*, 2018, **189**, 370–376.
40 P. Song, Y. Xiang, H. Xing, Z. Zhou, A. Tong and Y. Lu, *Anal. Chem.*, 2012, **84**, 2916–2922.
41 J. Wang, X. Wang, S. Wu, R. Che, P. Luo and C. Meng, *Biosens. Bioelectron.*, 2017, **87**, 984–990.
42 J. Pan, Q. Li, D. Zhou and J. Chen, *New J. Chem.*, 2019, **43**, 5857–5862.
43 J. Chen, S. Chen and F. Li, *Chem. Commun.*, 2017, **53**, 8743–8746.
44 Z. Zhang and I. M. Hsing, *Anal. Chem.*, 2017, **89**, 12466–12471.
45 Y. Lu, F. Luo, Z. Li, G. Dai, Z. Chu, J. Zhang, F. Zhang, Q. Wang and P. He, *Talanta*, 2021, **222**, 121686.

